Source of the Myocardial "Bite" Artifact in High Field Cardiac MRI

D. J. Anderson[1,2], J. M. Dendy[1,3], and C. B. Paschal[1,4]

[1]Department of Biomedical Engineering, Vanderbilt University School of Engineering, Nashville, TN, United States, [2]Vanderbilt University School of Medicine, Nashville, TN, United States, [3]Division of Cardiovascular Medicine, Vanderbilt University Medical Center, Nashville, TN, United States, [4]Vanderbilt University Institute of Imaging Science, Vanderbilt University, Nashville, TN, United States

Introduction

A "bite"-shaped signal void artifact is often seen in gradient echo MR images in myocardium along the infero-apical border of the heart. Two previous studies attempting to explain the cause of this artifact came to different conclusions. One suggested deoxygenated blood in the posterior vein of the left ventricle (PVLV) and other epicardial veins leads to a susceptibility gradient that causes the artifact [1]. The other suggested that the difference between lung and myocardial tissue susceptibility was responsible [2]. The present study assessed the relative effect of each possible cause via rigorous simulation.

Methods

Anthropometric phantoms were developed for use with a four step MRI simulation procedure. First, the object to be imaged was defined in terms of tissue types and morphology by modifying the phantom created by Zubal, et al. [3] to add a PVLV and coronary sinus (CS), specify blood as oxygenated or deoxygenated in appropriate locations, and interpolate the voxels to a more realistic size. Second, the digital object definition was converted to a matrix of susceptibility values. The susceptibility of bulk lung tissue was calculated as a weighted average of the susceptibilities of soft tissue and air. Since air has a near-zero susceptibility, multiplying the susceptibility of general soft tissue (-9.05 ppm) by 0.26, the density of inflated lung tissue [4], provides a reasonable estimate of the bulk lung susceptibility. Third, the susceptibility matrix was used to calculate static magnetic field perturbations using the Susceptibility-Voxel Convolution (SVC) method described by Yoder, et al. [5]. Fourth, the object definition and the calculated field perturbations were used to generate an image using the simulator developed by Yoder, et al. [5]. The simulator is based on the Bloch equations and allows for inclusion of the previously calculated field offsets and consequent intravoxel dephasing and signal mismapping throughout acquisition protocols. Images were simulated at 3 T with gradient echo scans using TE=8ms, TR=20ms, and θ=30°. Four different simulations were carried out to assess the effect of blood oxygenation in the PVLV and CS and presence of the heart-lung interface on myocardial signal.

Results

Results of the simulations shown in Figure 1 indicate that both susceptibility differences lead to signal losses in the area of the artifact with contributions from the PVLV being more localized to the "bite" area while lung tissue effects were stronger but more spatially distributed. The data support the conclusion that both differences together, rather than one or the other, are responsible for the artifact.

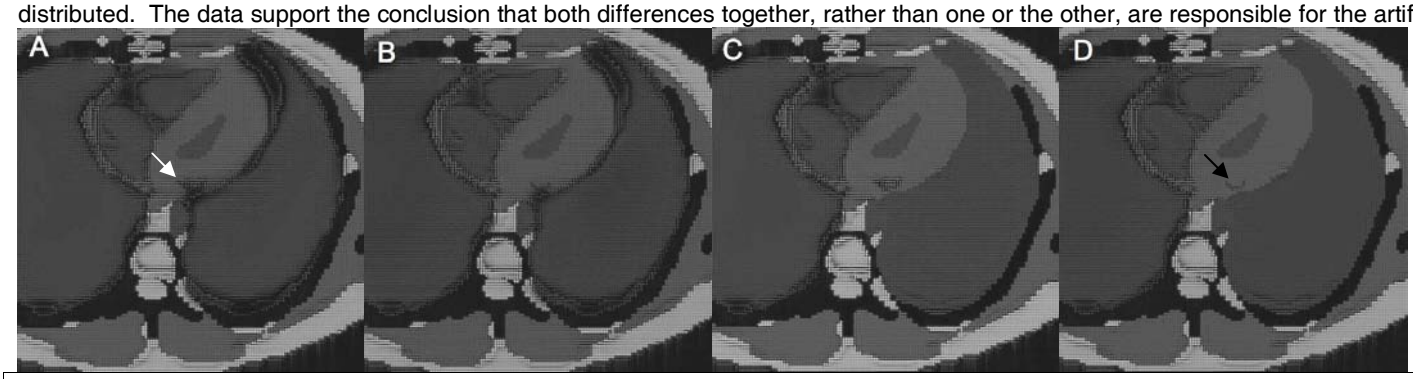

Figure 1. Simulation images showing variation in the "bite"-shaped artifact (white arrow) dependent on oxygenation of blood in the PVLV and CS and the susceptibility of the left lung. (A) Normal deoxygenated blood in the PVLV and CS and normal lung susceptibility produces the typical bite artifact (white arrow). (B) Normal lung susceptibility but with oxygenated blood in the PVLV and CS reduces the size of the bite artifact and results in 22% more signal in the area of the PVLV. (C) Normal deoxygenated blood in the PVLV and CS but with left lung susceptibility set to that of soft tissue results in reduced signal loss all along the myocardial-left lung interface. The bite artifact is present but less severe than in (A) or (B) with 67% more signal in the area of the PVLV compared to (A). (D) Putting oxygenated blood in the PVLV and CS and setting left lung susceptibility to that of soft tissue removes the artifact, leaving only the signal for oxygenated blood in the PVLV structure (black arrow). The signal in (D) is 72% greater than in (A), indicating that oxygenation of blood in the PVLV and CS affects the artifact on top of the stronger heart-lung interface effects.

Discussion and Conclusion

The simulator used in this study provides a "perfect" imaging system with homogeneous applied static and radiofrequency fields, perfect gradients, complete spoiling, no noise or motion, and no eddy currents. Field perturbations are supplied by the user based on the susceptibilities of the imaged object. Thus, realistic artifacts due solely to static magnetic field inhomogeneities are revealed. The results of this work show that susceptibility differences caused by deoxygenated blood in the PVLV and CS and the heart-lung interface lead to artifacts presenting as myocardial signal voids in simulated images of the human chest. The data support the conclusion that the susceptibility of deoxygenated blood in the PVLV and CS is responsible for the focal nature of the "bite"-shaped myocardial signal void, with the susceptibility gradient due to the heart-lung interface being a large, but more distributed, contributor to the artifact. This simulation technique is useful in investigating cardiac MRI artifacts that increase in severity at higher fields as well as investigating solutions such as possible application of shimming techniques or pulse sequence techniques.

References

(1) Reeder, S.B., et al. Magn Reson Med, 1998. **39**(6): p. 988-98. (2) Atalay, M.K., et al. Magnetic Resonance in Medicine, 2001. **45**: p. 341-3435. (3) Zubal, G., et al. July 31, 2001 [cited 2006 Nov.]; Available from: http://noodle.med.yale.edu/zubal/library.htm. (4) ICRU, *Tissue Substitutes in Radiation Dosimetry and Measurement*, in *Report 44 of the International Commission on Radiation Units and Measurements*. 1989, ICRU: Bethesda, MD. (5) Yoder, D.A., et al., *MRI Simulator with object-specific field map calculations.* Magnetic Resonance Imaging, 2004. **22**: p. 315-328.